UNDERSTANDING THE LONG-TERM EFFECTS OF ENVIRONMENTAL EXPOSURE ON ROOF REFLECTANCE IN CALIFORNIA

Meng-Dawn Cheng[1], William Miller[1], Joshua New[1], and Paul Berdahl[2]

[1]Oak Ridge National Laboratory, Oak Ridge, Tennessee, USA

[2]Lawrence Berkeley National Laboratory, Berkeley, California, USA

ABSTRACT

Cool-pigmented roofing systems could play an important role in the reduction of energy consumption. Cool roofs are those that show high reflectance of sunlight and are designed to retain the ability over time. Airborne particulate matter that settles on a roof can either reflect or absorb incoming solar radiation, dependent on the chemical content and size of the particles thereby affecting the ability of a roof to cool. These light scattering and absorption processes occur within a few microns of the surface, and can affect the solar reflectance of the roof. Contaminants collected from samples of roof products (i.e., coupons) exposed at seven California weathering sites were analyzed for elements and carbons to characterize the chemical profile of the particles soiling each roof sample and to identify those elements that degrade or enhance solar reflectance. The losses in solar reflectance varied from site to site and also varied at a give site based on the color of the coupon. The least drop in reflectance was observed in the alpine climate of McArthur while the largest drop occurred in sites near urban development. Light color samples were soiled after just one year of exposure. The darker color coupons did not show the same seasonal variations in solar reflectance as observed for the lighter colors. However, after an additional year of exposure the samples at all sites regained most of their solar reflectance due to rain and/or wind washing. The change of reflectance appears cyclical with the onset of seasons having more rainfall. Solar reflectance of the cool pigmented coupons always exceeded that of the conventional pigmented coupons. Climatic soiling did not cause the cool pigmented roof coupons to lose any more solar reflectance than their conventional pigmented

counterparts. The effect of roof slope appears to have more of an effect on lighter color roofs whose solar reflectance exceeds at least 0.5 and visually shows the accumulation of airborne contaminants. The thermal emittance remained invariant with time and location and was therefore not affected by climatic soiling. A thin-film deposition model was developed based on first principles, which simulates light interaction with a soiled substrate. This model was used in combination with the measurements to determine the solar absorption and reflectance of particulate matter at each of the sites calculated using the least squares fitting routines. Principal Component Analysis was used to determine the most important combinations of chemicals correlated with changes in solar absorption. The linear regression model identifies an approximate correlation using chromium, iron and elemental carbon concentrations. It appears that chromium ranks first, iron ranks second, and elemental carbon ranks third in importance to soil light absorption.

KEYWORDS

Absorption
Aerosols
Building Envelop
Cool Roof
Principal Component Analysis
Reflectance
Soot

INTRODUCTION

The long-term benefits of cool pigmented roofing systems (Akbari et al. 2004) can be compromised if a significant loss in solar reflectance occurs during the first few years of service life. Ultraviolet radiation, atmospheric pollution, microbial growths, acid rain, temperature cycling caused by sunlight and sudden thunderstorms, moisture penetration, condensation, wind, hail, and freezing and thawing are all thought to contribute to the loss of a roof's solar reflectance. Akbari and Konopacki (1998) and Miller et al. (2004) showed that in moderate to predominantly hot climates, an exterior roof surface with a high solar reflectance and high thermal emittance will reduce the exterior temperature and produce savings in comfort cooling. For predominantly heating-load climates, surfaces with moderate reflectance but low infrared emittance save in comfort heating. Determining the effects of climatic soiling on the solar reflectance and infrared emittance of cool color roofs is therefore very important for developing realistic claims of the net energy savings (cooling energy savings less heating penalty). Field data reported by Miller et al. (2002) suggests that the loss of roof reflectance is due to dust load and or biomass accumulation, which in turn is modulated by the climatic conditions. Biomass may be due to the growth of fungi and/or mold species that were transported by airborne particulate matter blown by the wind. Deposition of atmospheric particles and moisture accumulation on the roof provide suitable conditions for the colonization of the microbes.

It is plausible that the aged solar reflectance of roofs is affected by many factors including atmospheric deposition of soot particles and dusts (e.g., dirt, road dust, and soil particles). To investigate the issues in depth, characterization of the chemical and physical attributes of the deposited particles was conducted on roof samples collected from the diverse climates of the state of California. Results published by Berdahl et al. (2002) indicate "the long-term change of solar reflectance appears to be determined by the ability of deposited soot to adhere to the roof, resisting washout by rain." Samples studied were bare metal and polyvinyl chloride (PVC) roofing weathered for 18 years. Berdahl et al. (2002) attributed soot, also known as black carbon or elemental carbon, to be the primary cause of long-term reflectance loss. Other potentially important light absorbing particles are iron-containing minerals such as hematite.

The objectives of this paper are (1) document the drop in solar reflectance and the change in thermal emittance for roof products having cool color pigments, (2) characterize the particulate matter deposited on roof samples of different materials, (3) establish the relationship

between the deposited particulate matter and reduction of solar reflectance, and (4) quantify the contributions of the chemical composition of the particulate matter on the enhancement or loss of solar reflectance on a roof material.

MATERIALS AND METHODS

Weathering Sites in California

Seven sites in the diverse climates of California (Table 1) were selected for exposing painted metal, clay and concrete tile roof products with and without cool color pigments. Custom-Bilt Metal, Steelscape, BASF, MonierLifetile, US Tile, Maruhachi Ceramics of America (MCA), the Shepherd Color Company, American Rooftile Coatings, Metro Roof products, Elk Corporation, Certainteed and Owens Corning supported the initiative by field testing roof samples at their respective manufacturing facilities (Table 1) and/or by providing roof products for this study. The California population is expanding rapidly in the Central Valley and around the LA basin, and the sites with Custom-Bilt (Sacramento) and Elk (Shafter) capture the effects of weather, urban pollution and the expanding population. These areas reflect the market for new homes. Weathering sites with Steelscape, BASF and MCA are located in existing densely populated areas of the San Francisco basin and LA, and represent the market for re-roofing existing homes. Samples were also exposed near weather stations maintained by the California Irrigation Management Information System (CIMIS, http://www.cimis.water.ca.gov/). Sites in McArthur and El Centro, CA. were selected for acquiring exposure data in the more extreme climates. McArthur is located in the moderate alpine climate of northern California (climate zone 16); El Centro is in the extremely hot desert climate of southern California bordering the Arizona state line (climate zone 15). Table 2 locates each weathering site and provides the closest CIMIS station to each weathering site. Solar reflectance (SR) of the new and aged samples is also provided in Table 2 for the samples used for elemental contaminant determinations.

Exposure Racks

All roof samples were installed in exposure rack assemblies, which are 1.68-m high by 2.74-m long, and divided into three sub-frames having respective slopes of 5.08-, 10.16- and 20.32-cm of rise per 30.48-cm of run (i.e., slopes of 9.5°, 18.4° and 33.7°). Each sub-frame can hold two sub-assemblies that are designed to have 6 rows of samples with 86.36-cm of usable space in each row. Sample size is 8.89-cm by 8.89-cm, a size that LBNL's spectrophotometer[1] can easily accommodate for measuring the solar reflectance at discrete wavelengths. Finally all exposure rack assemblies were oriented facing south for full exposure to natural sunlight and weathering (Fig. 1).

Instruments

A Device and Services solar spectrum reflectometer was used to measure the solar reflectance (total hemispherical reflectance over spectrum of sun's energy) of the roof samples. The device uses a tungsten halogen lamp to diffusely illuminate a sample. Four detectors, each fitted with differently colored filters, measure the reflected light in different wavelength ranges. The four signals are weighted in appropriate proportions to yield the solar reflectance. The device was proven accurate to within ±0.003 units (Petrie et al. 2000) through validation against the ASTM E-903 method (ASTM 1996). However, because the cool pigmented roof products exhibit high infrared reflectance, some of the field samples were measured at LBNL using their spectrophotometer to validate the portable Device and Services reflectometer. The average absolute difference between the portable reflectometer and the spectrophotometer was about 0.02 points of reflectance with the spectrophotometer consistently reading lower than the reflectometer (as example, the reflectometer measured a solar reflectance of 0.741 for a IR painted metal while the spectrophotometer measured 0.73).

The impact of emittance on roof temperature is as important as that of reflectance. A portable Device and Services emissometer was used to measure the thermal emittance using the procedures in ASTM C-1371 (ASTM 1997). The device has a thermopile radiation detector, which is heated to 82.2°C (180°F). The detector has two high-ε and two low-ε elements and is designed to respond only to radiation heat transfer between itself and the sample. Because the

[1] Perkin-Elmer Lambda 900

141 device is comparative between the high-ε and the low-ε elements, it must be calibrated in situ
142 using two standards, one having an emittance of 0.89, the other having an emittance of 0.06.
143 Kollie, Weaver, and McElroy (1990) verified the instrument's precision as ±0.008 units and its
144 accuracy as ±0.014 units in controlled laboratory conditions.
145

146 ## *Analytical Method for Elemental Contaminants of Roofing Samples*

147 Contaminants were swabbed from the concrete and painted metal coupons identified in
148 Table 2. The samples from a single site were removed from the exposure racks, wrapped in
149 aluminum foil, stored in a zip lock bag and sent airfreight back to ORNL. Each sample was
150 placed in a laboratory-sonicating[2] bath filled with 800 mL of distilled water held at room
151 temperature. After 20 min, the sample was removed from the bath using sterilized stainless steel
152 forceps. The water suspension was then poured into a filtration system with vacuum applied to
153 filter the suspended particulate onto the filters. The solution was divided into two 400-mL
154 aliquots. One 400-mL sub-sample was filtered through a 47-mm diameter nylon filter
155 (OSMONIC, Inc., 0.1μm pore size) that was subsequently analyzed for selected metal
156 composition by a certified analytical lab. The other 400-mL sub-sample was passed through the
157 same filtration system through a 47-mm diameter glass fiber filter (Whatman 934-GF). About
158 100 mL of additional deionized water was used to rinse off any particulate matter (PM) that
159 remained on the samples. All the filters were placed in a laboratory desiccator and held overnight
160 at room temperature before being analyzed. For quality control, 400 ml of deionized water was
161 filtered through a nylon filter to create an analytical blank of metal species. A glass fiber blank
162 was created similarly for carbon analysis. The filtration apparatus was rinsed three times using
163 deionized water in between different filtration runs.
164 Inductively Coupled Plasma (ICP) – Atomic Emission Spectrometry (AES) was used for
165 analysis of the metal content on the filters. Metal concentrations in the deposited PM that
166 exceeded those detected for blank values were reported. The carbon content was analyzed for
167 total, elemental, and organic carbon by the Sunset Laboratory[3], Inc., Portland, OR. Three
168 samples, each 1-square cm, were punched out from a 47-mm diameter quartz filter and analyzed

[2] Sonicating agitates the bath using high-frequency sound waves.
[3] The Sunset instrument is capable of analyzing carbon content of a filter sample using the temperature and oxidation profiles of particulate carbonaceous species to define organic vs. elemental carbon (i.e., OC vs. EC). The total sum of OC and EC is called the total carbon of a sample.

by the instrument, and the average of the triplicate was assigned as the carbon concentration for the sample. If the coefficient of variation of the triplicate concentration is greater than ±5%, the sample is considered as non-uniform deposition and the result may be discarded. In this study all the samples met the precision requirement and were retained in the subsequent data analysis. We did not analyze for soluble materials that might dissolve into the solution, because our prior experience shows the metallic and carbon contents in the solution were negligible compared to those on the suspended particles. It is possible that numerous wet-dry cycles occurred on the sample coupons over the years might have leached out the dissolvable materials leaving us not much to find in the solution.

Field Measurements

Coupons of concrete and clay tile and painted metal roof samples were exposed to the atmosphere in six of California's sixteen climate zones. Contaminant samples were collected after 1.6 and 4.1 years of exposure for the coupons identified in Table 2. The measurements of solar reflectance and thermal emittance are reported herein to view the time dependence of climatic soiling and later, in the contaminants section, the impact of the various contaminants on the loss of solar reflectance.

RESULTS AND DISCUSSION

Effects of Soiling on Roof Samples in the Field

The Regal white painted PVDF coupon steadily lost solar reflectance over the first year of exposure (Fig. 2). The loss varied from site to site with the least drop observed at McArthur (4% after one year) and the worst occurring in the more desert-like areas of Colton and Meloland (23% after one year). The exposure rack in Colton is roof-mounted while the one in Meloland is ground mounted (Table 1), but the change in the roof's solar reflectance after one year of exposure is very similar between the two sites. Visible inspection of the Regal white painted metal exposed at Shafter [medium sloped rack (10.6-cm rise per 30.48-cm run)] showed that the sample was soiled by airborne debris after one year of exposure (Fig. 3). However, after an

199 additional 8 months of weathering the samples at all sites regained most of their solar reflectance
200 (average SR loss of only 6% from starting SR value). Meloland and Shafter had less than1.27-cm
201 of rainfall from Aug 04 through April 05; however, McArthur, Corona, Colton, Sacramento and
202 Richmond had two consecutive months in early 2005 with rains exceeding 12.7-cm per month.
203 The average winds remained steady at about 1.79 to 2.24 m s^{-1} over the entire exposure period at
204 all sites. Hence the results are showing that the loss of reflectance is remedied in part by the
205 combination of precipitation and wind sweeping or simply wind sweeping in the drier climates of
206 El Centro and Shafter.
207 The darker charcoal gray coupon did not show the same seasonal variations in solar
208 reflectance as the lighter coupon because its solar reflectance is roughly half that of the white
209 painted metal (Fig. 4). Dusts tend to lighten darker colors and the soiling of the charcoal gray
210 coupon slightly increased solar reflectance. Coupons of the same color but having conventional
211 pigments (labeled standard in Fig. 2 and 4) have lower solar reflectance than do the cool
212 pigmented colors during the entire exposure period. The result is important because climatic
213 soiling did not cause the cool pigmented colors to degrade more than that observed for the
214 conventional pigmented colors. Therefore the cool pigmented painted metals performed as well
215 as their counterparts. Further, the infrared reflective pigments boost the solar reflectance of a
216 dark more aesthetically pleasing color to about 0.3 to 0.4 (view standard versus cool pigments at
217 start of exposure Fig. 4) and results for the charcoal gray painted metal shows only about a 3%
218 drop in solar reflectance over about 4 years of exposure. Climatic soiling had little effect on the
219 solar reflectance of clay and concrete tile (Fig. 5). Dusts appear to lighten the darker Terra Cotta
220 color.
221 The effect of roof slope becomes somewhat significant for coupons exceeding an initial
222 solar reflectance of 0.50, as observed for the Regal white painted metal coupons displayed in Fig.
223 6. As stated the coupons collect dust with the worst soiling occurring for samples exposed in
224 Meloland, Colton, Corona and Shafter. The crisp and clear alpine climate of McArthur continues
225 to show the lowest loss of reflectance (Fig. 6). The drop in solar reflectance diminishes slightly
226 as roof slope increases for samples at Meloland and McArthur. Also the darker more
227 aesthetically pleasing roof colors do not show the trend. The darker charcoal gray coupon shows
228 slight increases in solar reflectance with time in El Centro and in Colton because of the
229 accumulation of dusts that tend to lighten a darker color. Therefore the effect of roof slope

appears more academic and its affect is secondary as compared to the soiling by airborne dust debris. It is also important to again point out that the cool pigmented colors maintain their solar reflectance as well as their conventional pigmented counterparts.

The thermal emittance of the painted metal, clay and concrete tile coupons has not changed much after 4 years of exposure in California (Table 3). Miller et al. (2004) and Wilkes et al. (2000) both observed little variation in the thermal emittance of painted and or coated surfaces. Consistent with reported findings, the thermal emittance did not vary from site-to-site nor did it change with time for these painted products. Thermal emittance of metals is strongly dependent on surface properties. Unpainted metals will over time oxidize; the metal oxide surface layer increases the thermal emittance (Miller and Kriner, 2001). However, the paint finishes applied to PVDF metal and clay and concrete tile are very durable and there is therefore no adverse weathering effects observed for the thermal emittance of painted roof products. In summary the results suggests that the losses in solar reflectance due to soiling occur after at least 2 to 3 years of exposure.

Contaminants Measured on the Roof Samples

Fig. 7 (data after 1.63 years of exposure) and Fig. 8 (data after 4.1 years of exposure) display the concentration of elements and the variation of these elements across the weathering sites. At some sites only one sample was pulled, while at another site several samples were pulled just to obtain a sufficient quantity of contaminants (Table 2). All elements shown on the X-axis of each plot are those whose concentrations were higher than the method's detection limits and above the blank values.

Coupons pulled after 4.1 years of exposure (Fig. 8) and those pulled after only 1.6 years of exposure show similar contaminant concentrations (Fig. 7). Many of the metals analyzed for all sites appear to be of crustal origins such as road dusts, soil, and or rock debris. Sulfur content in the roof samples was not large, which may be attributed to the absence of coal-fired power plants in California. Sulfur (S) was lowest at McArthur possibly because of its rural location while at all other sites the concentration of S was about the same. Calcium is found to be in rather high abundance, except for the remote McArthur site in northeastern California. The elements aluminum, silicon, potassium, titanium, iron and barium (Al, Si, K, Ti, Fe and Ba) are typically associated with soil dust and their respective concentrations are similar across all

weathering sites. Greater variations are observed with anthropogenic elements such as vanadium, chromium, nickel, zinc, and lead (V, Cr, Ni, Zn, and Pb). Generally the clear alpine climate of McArthur yielded the lowest or near lowest concentration of these elements emanating from anthropogenic emissions.

OC values are higher than EC values for all sites. The McArthur site had the least amount of EC per unit area. Plants and vegetations are excellent sources of emission of organic compounds that could be detected as OC, if the compounds or their reaction products were condensible that could be found on particulate matter. On the other hand, elemental carbons (e.g., soot) are emitted from combustion sources such as vehicle engine exhausts. We thus attributed the observed higher EC values in Shafter, Richmond and Sacramento to potential contributions by traffic and vehicle emissions at the sites. The traffic volume around the McArthur site area is much less than other areas, but McArthur is in a forest area where biogenic emissions might be significant. This resulted in higher OC than EC, and the data reported here support this understanding.

To further investigate the sources of carbon content in aerosol particles, we computed the ratios of EC to OC for the seven sites based on the data shown in Figs 7 and 8. Appel et al. (1976), Turpin and Huntzicker (1995), and Strader et al. (1999) have successfully used the EC/OC ratio to identify whether the carbon in aerosol was primary or secondary in content. If the EC/OC ratio is low and correlation between OC and EC is high, the carbon is likely originated from direct emissions. Average EC/OC value reported by Appel et al. (1976), Turpin and Huntzicker (1995), and Strader et al. (1999) is about 0.48 in winter, 0.32 in spring, and 0.18 in summer. The EC/OC ratios computed for the seven sites were all smaller than 0.18, much smaller than 0.48. These results suggest averaged over the 1.6- and 4.1-year exposure periods, the carbon contents found on PM deposited at these sites were driven primarily by sources such as biogenic emissions and or forest or local brush fire rather than photochemical conversion. The results presented in Figs 7 and 8 indicate two major contributors of particulate matter: crustal sources and traffic activities.

Miller et al. (2006) conducted linear regression analysis to determine the important chemical elements that contributed to the loss of roof reflectance using only the 1.6-year exposure data (the 2005 data) was available from the CA weathering sites. Results showed statistically that Cr, Cu, Mn, Mg, Ni, Na, S, V, and EC had little contribution to the change of

292 solar reflectance. Al and OC contributed to the increase of solar reflectance values found at the
293 sites, and Ca, Fe, K, Si, and Zn could contribute to the degradation of solar reflectance measured
294 on the roof samples.
295 Aluminum oxide has a refractive index of about 1.7, and its particles can thus be
296 reflective in the visible to infrared region. Organic carbon, OC, is a highly complex mixture of
297 materials containing carbon that can be detected in the form of CO_2 when burned. OC is well
298 known to be a reflective component of aerosol particles [see Novakov and Penner (1993) in
299 http://eetd.lbl.gov/newsletter/nl17/blackcarbon.html, for example] due to its ability to scatter
300 light. OC absorbs at short wavelengths (UV and blue), but is reflective at longer wavelengths.
301 EC is commonly referred to as black carbon or soot and is believed to be a significant factor in
302 the loss of a roof's solar reflectance (Berdahl et al., 2002).
303 The second set of elemental contaminants collected after 4 years of exposure (2008 data)
304 were statistically analyzed with and without the contaminant data collected after just 1.6 years of
305 exposure (2005 data). A principal component analysis (PCA) test identified the parameters that
306 best describe the solar reflectance of the roof samples. When each data set was analyzed
307 individually, PCA resolved both data sets to show two components. The component-loading
308 pattern is different from one set to another due to the number and elements used in each analysis.
309 Nevertheless, one component is always related to dust characterized by the chemical species Al,
310 Ca, Fe, K, Si, OC. Br is also observed and its presence is likely to come from the sea salt. The
311 other principal component is of anthropogenic origin and was identified as Cu, Sb, and Zn.
312 Corona showed the greatest amounts of anthropogenic contaminants possibly because of
313 increased industrial activities from 2005 to 2008.
314 The role of elemental carbon (i.e., soot) if in significant content in aerosols has dramatic
315 effects on the loss of solar reflectance. Berdahl (2006) shows the expected solar reflectance and
316 visible reflectance as a function of soot concentration. The OC and EC amounts measured in mg
317 per unit area in centimeter squared at these seven sites are shown in Table 4. The largest EC per
318 unit area for coupons exposed for 1.63 years was found at Richmond; however, for the samples
319 exposed for 4.06 years, all sites with exception of Richmond had increased deposition of EC.
320 Previous reporting by Miller et al. (2006) stated that EC was found in too small concentrations to
321 be a significant contributor in reducing surface reflectance at all seven sites in California. The

more recent data shows that EC may indeed affect the solar reflectance of the roof samples and could be used to describe the subsequent losses.

A Simple Model for a Soiled Substrate

An increase in solar reflectance requires the addition of light-scattering particles. For example, a white powder increases the reflectance of a black or gray substrate. The ability of a particle to scatter light is proportional to the difference in refractive index of a particle and that of the surrounding medium as described by $(n_{pl}-n_o)^2$ where n_{pl} is the real refractive index of the particle and n_o is the refractive index of the surrounding medium. As example, many minerals and organic substances have refractive indices in the range of [1.3 to 1.8] and therefore in air (n_o = 1) cause light scattering.

Suppose there is a soil layer with absorption *a*, reflectance *r*, and transmittance *t* on a substrate with a clean reflectance denoted Ro and one wishes to compute the soiled substrate reflectance R (see Fig. 9). A photon interacts with the soiled substrate in one of three ways. In the first process the photon can be reflected directly by the soil (Process 1); the photon can be transmitted through the soil, reflected by the substrate, and transmitted again by the soil (Process 2); or the photon can be transmitted twice, reflected from the substrate twice, and reflected by the underside of the soil (Process 3). Therefore summing the different ways a photon can be reflected as demonstrated in Fig. 9 yields a formulation for the reflectance of the soiled substrate as:

$$R = r + t^2 R_O + t^2 R_O^2 r + \cdots \qquad (1)$$

Since an incident photon must be absorbed, reflected, or transmitted, we know that $a + r + t = 1$. We can therefore eliminate *t* in our equation in favor of "*a*" and "*r*" if we assume the deposited particle layer or soil layer on a roof sample is thin ("*a*" and "*r*" are small compared to unity) so quadratic and higher powers of "*a*" and "*r*" are small and can be discarded[4]. It follows then that the change in reflectance R of the soiled substrate is given, to first order in "*a*" and "*r*", by:

$$R - R_O = -2R_O a + (1 - R_O)^2 r \qquad (2)$$

[4] If the soil layer is not thin, it can be divided into thin sublayers and the current method can be used recursively, leading to more complex equations.

Thus increasing the soil absorption "*a"* reduces the reflectance R of the soiled substrate while increasing the soil reflectance "r" increases R. The importance of "a" diminishes if Ro is small, and "r" will be less important if Ro is close to unity.

Model Limitations

The proposed model neglects the angular distributions of the radiant energy. A two-stream approximation was assumed, keeping track only of whether the radiation is traveling up or down. Physically, radiation traveling normal to the soil layer has a shorter path length than radiation traveling obliquely. If one associates the absorption "a" with a measured Lambert-Beer's law absorption[5], there is an ambiguity as to the correct path length and a corresponding ambiguity in "a" by about a factor of 2.

The model also neglects the spectral distributions of the radiant energy. Spectral components of the absorption are likely to be larger at short wavelengths, since most materials absorb more strongly in the visible and UV compared with the near infrared. Thus the parameters "a" and "r" should be understood as average values over the solar spectrum. Note that for "a" =0.2, the spectral value of "a" may still be rather large at short wavelengths, invalidating our approximation that "a" << 1. The simple model assumes a uniform layer of soil. In principal, it may need to describe the varying thickness of the soil layer.

Computed "a" and "r" Values for Soiled Substrates

Despite the above-mentioned limitations in the model of a soiled substrate, the method's strength stems from its simplicity. Based on Eq. (2), if we have measured values of both R and R_0 for two samples with differing R_0 but the same soil layer, then we can compute values for "a" and *r*. Now in most cases, we have measurements with a dozen or more samples with the same soil layer, so we can refine the determination of "a" and "r" by the least-squares fitting. The results for the "a" and "r" coefficients of polyvinylidene-fluoride (PVDF) painted metal roof samples at all slopes are listed in Table 5 and clay roofs at all slopes are listed in Table 6.

[5] The Lambert-Beer law assumes a logarithmic dependence between the transmission of light through a soiled substrate and the product of the path length of light with the absorption coefficient of the substrate.

Computations were made for all CA sites and all times where solar reflectance measurements were collected in the field and passed the Grubb's statistical[6] test for outliers.

To show the quality of the fits, plots of the absolute change in reflectance of the coupons (Fig. 10) are computed using Eq. 2 with the "a" and "r" coefficients in Table 5 and superimposed on the reduced data for coupons exposed at the various sites over the span of approximately four years. The optimal values for the "a" and "r" terms (Table 5) were calculated for coupon reflectance data measured at a respective time. On the Y-axis (Fig. 10) the coupon's solar reflectance R less the new coupon's initial solar reflectance Ro is plotted as a function of Ro. Dark samples (small Ro) have an increased reflectance and light samples (large Ro) have a decreased reflectance. The ordinate at R-Ro=0 marks zero reflectance change, and the curve intersects this line at Ro = 0.32. Thus a sample with Ro=0.32 will be unchanged in reflectance by added dust. This critical value for Ro is actually a function of *a/r*. Larger "a" leads to a darker surface, while a smaller "a" yields a lighter surface. In summary, in the fitting process, both parameters "a" and "r" are determined by minimizing the mean square deviation of $R-R_0$ from the fitted line. It should be noted that clay roofs averaged 34% higher soil absorption "*a*" coefficient than yielded by the PVDF-painted metal roofs, highlighting material-specific soiling dynamics. Likewise, compared to average low-slope soil absorption, mid-slope had an 11% reduction and steep-slope had a 16% reduction. The observation helps again confirm that there is some enhanced washing of the coupons at steeper slopes resulting in higher reflectivity over time.

Principal Component Analysis (PCA)

Additional statistical techniques were used to investigate the contribution of individual elements or combinations of elements on solar reflectance. First, principal component analysis was used to resolve the combinations of elements that account for the variability of the contaminant concentration data as well as correlation to soil absorption and reflectance. Second, linear fits were utilized to determine which elements or combination of elements is best for predicting soil absorption and reflectance. Each analysis is discussed in more detail below, and is

[6] Grubbs' test was used to detect and eliminate outliers in the data set.

based upon the contaminant data from the five sites and between the two time periods whenever concentrations exceeded the detection threshold shown in Table 7.

The soil absorption "a" and the soil reflectance "r" was included in a correlation matrix and again analyzed using PCA that effectively treats "a" and "r" as variables in the same manner as the included chemical contaminants. The first three eigenvectors together accounted for 78.3% of the variation with the "a" and 78.5% of the correlation with *r*. An orthonormal basis vector was derived and utilized for the Varimax-rotated components in order to precisely align eigenvectors with "a" or *r*. This maximizes the correlation of a given contaminant element directly with "a" or *r*. The Varimax rotation was applied to the retained principal components to rationalize the eigenvectors and practically limits the contributions from elements that exhibit only minor influences on the principal components. The element loadings for each rotated eigenvector are shown in Table 8. These loadings are indicative of the relative importance of each chemical in correlation to "a" or "r" with decreasing importance for subsequent eigenvectors.

The elements with the highest loadings were: Fe, OC, Ca in the rotated vector 1 for "a", Fe, OC, Ca, Si for the vector 2, and Fe, OC, Zn, and Si for the vector 3. The highest loadings for "r" are Fe, OC, Ca, and Si for vector 1, Fe, OC, Ca, Si for vector 2, and Fe, OC, Zn, and Si for the vector 3. The major eigenvectors for both "a" and "r" had per-element loading factors in the following order: Fe, OC, Ca, Si, and Zn. These eigenvector loadings correspond well to the elements with the largest concentrations present in the soil.

Linear Regression

Linear regression was utilized to estimate the soil absorption "a" and reflectance *r*. Fits were generated for one, two, and three contaminants to determine which combinations best predicted "a" or "*r*". As another example, the best 2-element prediction for the soil absorption "a" and reflectance "r" is given in Table 9 by the following two fits:

$$a = 0.00158 - 0.00669[Cr] + 0.02899[Si] \quad (3)$$

$$r = 0.00208 - 0.05439[Cr] + 0.04609[Si] \quad (4)$$

where

$[Cr]$ = the concentration of Cr in mg m^{-2}, and

434 $[Si]$ = the concentration of Si in mg m^{-2}.

435

436 Linear regression and exhaustive search of all possible k-element contributions was used
437 to find the optimal linear combination of elements for "a" and "r" in the data. With the small
438 chemical data set, it is important to note that the confidence in the statistical results discussed
439 above is limited. We thus include a physical chemistry-based interpretation to corroborate
440 elemental contaminant effects.

441 The relatively abundant transition metals Fe, Mn, Cu, Cr, have colored or black oxides
442 that reduce roof reflectance. Of these elements, iron was the most abundant contaminant found
443 on the soiled coupons. The presence of iron in mineral dust is accompanied by a reddish
444 (hematite) or brownish tint (FeOOH). Hematite is a strong absorber of the short wavelength part
445 of the solar spectrum (300 to 550 nm) with a coefficient of about 4 m^2 g^{-1} (Levinson, Berdahl
446 and Akbari, 2005). Thus such a hematite layer could absorb a measurable portion (~20 %) of the
447 short wavelength component. Most of the iron present is unlikely to be in the form of pure iron
448 oxides, but rather in mineral particles containing other oxides like Si, Al, Ca, etc. as well.

449 Plotting iron concentration against the soiled absorption "a" for data measured after 4.1
450 years of exposure revealed a potential correlation between the optical absorption "a" and the iron
451 concentration, Fig. 11a. Here the elemental compositions and the *a*-values are from Table 7. The
452 estimation of "a" was improved by including the effect of chromium compounds (Fig. 11b). Note
453 that the inclusion of chromium concentration reduced the least-squares fit coefficient for iron.
454 Finally, a three-term fit for soil absorption "*a"* was used to incorporate elemental carbon [C]
455 concentration as well. This final fit yields a result with an rms deviation of only $\Delta a = 0.008$. The
456 units of the coefficient are given in m^2 g^{-1}: 1.52 for Fe, 19.9 for Cr, and 15.8 for C. Table 10
457 summarizes the status of the absorption coefficients.

458 Furthermore, the earth's crust contains about 5% Fe by weight, and 0.01 % Cr. The ratio
459 [Cr]/[Fe] might be expected to be ~ 0.002, if the deposited particulate matter consists of
460 primarily crustal material. The data in Table 7 show that at 4.1 yr this ratio is 0.03 – 0.2, much
461 larger than 0.002. We thus infer that most of the chromium is of anthropogenic origin.
462 Kirchstetter et al. (2004) reported that the absorption of soot is approximately 14 m^2 g^{-1} at 550
463 nm, which is not far from our value, 15.8. Berdahl, Akbari and Rose (2002) estimate about 8 m^2
464 g^{-1}. The relative closeness of our new coefficient for carbon to that of published values of soot

465 reinforces the interpretation that soot is indeed the cause. Babin and Stramsky (2004) studied
466 light absorption by mineral particles suspended in water. They identified iron compounds as
467 quite important and found that the absorption at 440 nm was in the range of 1 to 4 m^2 per gram
468 of iron. Our result shows the absorption by Fe is 1.58 m^2 g^{-1}. This absorption was even stronger
469 in the ultraviolet and disappeared near 600 nm. A derived rough estimate for the solar-spectrum-
470 averaged value of Fe absorption is 0.2 – 1.0 m^2 g^{-1}.

CONCLUSIONS

Seven sites in the arid, alpine, urban populated and also the cool, humid climates of California were selected for exposing painted PVDF metal, clay and concrete tile samples with and without cool pigmented colors. The losses in solar reflectance varied from site to site and also varied at a give site based on the color of the coupon. The least drop in reflectance was observed in the alpine climate of McArthur while the largest drop occurred in sites near urban development. Visible inspection of the Regal white PVDF metal exposed at Shafter showed the sample was soiled with airborne debris and had lost 24% of it initial solar reflectance after just one year of exposure. The darker color coupons did not show the same seasonal variations in solar reflectance as observed for the lighter colors. However, after an additional 18 months of exposure the samples at all sites regained most of the solar reflectance due to rain washing. Field data show the loss of reflectance is cyclic with the onset of seasons having more rainfall. Solar reflectance of the cool pigmented coupons always exceeded that of the conventional pigmented coupons. Climatic soiling did not cause the cool pigmented roof coupons to lose any more solar reflectance than their conventional pigmented counterparts. The effect of roof slope appears to have more of an effect on lighter color roofs whose solar reflectance exceeds at least 0.5 and visually shows the accumulation of airborne contaminants. However, precipitation and or wind sweeping helps restore most of the initial solar reflectance. The thermal emittance remained invariant with time and location and was therefore not affected by climatic soiling.

The roof samples collected at seven California sites after 1.6 years and 4.1 years of exposure have been analyzed for metals and carbons. The chemical profile of the particles collected by each roof sample was obtained and reported for the seven sites. Cross-correlation analysis of the seven chemical profiles shows a clear separation between the rural and urban/industrial sites and correlation among sites in Southern California. Many of the contaminants were of crustal origin such as road dusts, soil and or rock debris. Iron was the most abundant contaminant found on the soiled samples. Higher elemental carbon concentrations were observed after 4.1 years of exposure than observed for 1.63 years.

PCA showed that the loss of solar reflectance of the field samples could be explainable by two independent factors that were likely to be dust and anthropogenic sources. Both factors explain over 85% of the data variation. We attempted to identify the elements that contribute to the loss or enhancement of solar reflectance by performing the linear least-square fit to the data.

502 We found that chromium, iron and elemental carbon were the major contributors to the change of
503 solar reflectance on the soiled samples that have been exposed to the elements for 4.1 years.
504
505

ACKNOWLEDGEMENTS

Funding for this project was provided by the California Energy Commission's Public Interest Energy Research program through the U. S. Department of Energy under contract DE-AC03-76SF00098. The elemental composition of particles was analyzed by the analytical chemistry services at the DOE Y12 complex using ICP-AES instrument. Oak Ridge National Laboratory is managed by UT-Battelle, LLC, for the U.S. Dept. of Energy under contract DE-AC05-00OR22725.

DISCLAIMERS

Mention of the trade names, instrument model and model number, and any commercial products in the manuscript does not represent the endorsement of the authors nor their employer, the Oak Ridge National Laboratory or the US Department of Energy.

NOMENCLATURE

CIMIS	California Irrigation Management Information System
CMRC	Cool Metal Roof Coalition
AISI	American Institute of Steel Industries
NamZac	Galvalume Sheet Producers of North America
MBMA	Metal Building Manufacturers Association
MCA	Metal Construction Association
NCCA	National Coil Coaters Association
PVC	Polyvinylchloride thermoplastic membranes
SR	Solar reflectance
TE	Thermal emittance
PM	Particulate matter

REFERENCES

Akbari,H., P. Berdahl, R. Levinson, R. Wiel, A. Desjarlais, W. Miller, N. Jenkins, A. Rosenfeld, C. Scruton (2004) Cool Colored Materials for Roofs, *ACEEE Summer Study on Energy Efficiency in Buildings.* Proceedings of American Council for an Energy Efficient Economy, Asilomar Conference Center in Pacific Grove, CA, August.

Akbari, H., Konopacki, S.J. 1998. "The Impact of Reflectivity and Emissivity of Roofs on Building Cooling and Heating Energy Use," in Thermal Performance of the Exterior Envelopes of Buildings, VII, proceedings of ASHRAE THERM VIII, Clearwater, FL., Dec. 1998.

ASTM. 1997. Designation C 1371-97: Standard Test Method for Determination of Emittance of Materials Near Room Temperature Using Portable Emissometers. American Society for Testing and Materials, West Conshohocken, PA.

_____. 1996. Designation E903-96: Standard Test Method for Solar Absorption, Reflectance, and Transmittance of Materials Using Integrating Spheres. American Society for Testing and Materials, West Conshohocken, PA.

Appel, B. R., P. Colodny, and J. J. Wesolowski (1976) Analysis of Carbonaceous Materials in Southern California Atmospheric Aerosols, Environ. Sci. Technol., 10: 359-363.

Babin, M., and D. Stramsky, Variations in the mass-specific absorption coefficient of mineral particles suspended in water (2004), *Limnol. Oceanogr.,* 49(3), 2004, 756–767.

Berdahl, P., H. Akbari, and L. S. Rose (2002) Aging of Reflective Roofs: Soot Deposition, *Appl. Opt.*, April 2002 Vol. 41, No. 12, 2355-2360.

Berdahl, P., H. Akbari, R. Levinson, and W. A. Miller (2008) Weathering of Roofing Materials-An Overview, Construction and Building Materials, Vol 22: 423 – 433.

Kirchstetter TW, Novakov T, Hobbs PV. Evidence that the spectral dependence of light absorption by aerosols is affected by organic carbon. J Geophys Res-Atmos 109(d21): D21208; 12 November 2004.

Kollie, T. G., F.J. Weaver, D.L. McElroy. 1990. "Evaluation of a Commercial, Portable, Ambient- Temperature Emissometer." Rev. Sci. Instrum., Vol. 61, 1509–1517.

Levinson, R, P. Berdahl, and H. Akbari (2005) Solar spectral optical properties of pigments – part II: survey of common colorants, Sol. Energy Mater. Sol. Cells 89, 351-389 (2005), Fig. 1, Film R03.

Miller, W.A., Cheng., M.D., Pfiffner, S., Akbari, A., Berdahl, P. and Levinson, R. (2006) Composition and Effects of Atmospheric Particles on the Performance of Steep-Slope Roofing Materials, Task Report to the California Energy Commission.

Miller, W.A., A. Desjarlais, D.S. Parker and S. Kriner (2004) Cool Metal Roofing Tested for Energy Efficiency and Sustainability, Proceedings of CIB World Building Congress, Toronto, Ontario, May 1-7, 2004.

Miller, W. and B. Rudolph (2003), Exposure Testing of Painted PVDF Metal Roofing, Report prepared for the Cool Metal Roof Coalition.

Miller, W.A., Cheng, M-D., Pfiffner, S., and Byars, N. (2002) *The Field Performance of High-Reflectance Single-Ply Membranes Exposed to Three Years of Weathering in Various U.S. Climates*, Final Report to SPRI, Inc., Aug., 2002.

Miller, W. A., and Kriner, S. 2001. "The Thermal Performance of Painted and Unpainted Structural Standing Seam Metal Roofing Systems Exposed to One Year of Weathering,"

in Thermal Performance of the Exterior Envelopes of Buildings, VIII, proceedings of ASHRAE THERM VIII, Clearwater, FL., Dec. 2001.

Novakov, T. and Penner, J.E. (1993) Large Contribution of Organic Aerosols to Cloud-Condensation-Nuclei Concentrations, *Nature*, 365, 823- 826.

Petrie, T. W., A.O. Desjarlais, R.H. Robertson and D.S. Parker. 2000. Comparison of techniques for in-situ, non-damaging measurement of solar reflectance of low-slope roof membrane. Presented at the 14th Symposium on Thermophysical Properties and under review for publication in International Journal of Thermophysics, Boulder, CO; National Institute of Standards and Technology.

Strader, R., P. Lurmann, and S. P. Pandis (1999) Evaluation of Secondary Organic Aerosol Formation in Winter, *Atmos. Environ*., 33: 4849-4863.

Turprin, B. J. and J. J. Huntzicker (1995) Identification of Secondary Organic Aerosol Episodes and Quantitation of Primary and Secondary Organic Aerosol Concentrations during SCAQS, *Atmos. Environ*., 29: 3527-3544.

White DC, Davis WM, Nickels JS, King JD, Bobbie RJ. 1979. Determination of the sedimentary microbial biodensity by extractable lipid phosphate. Oecologia 40: 51-62.

Wilkes, K. E., Petrie, T. W., Atchley, J. A., and Childs, P. W. (2000) Roof Heating and Cooling Loads in Various Climates for the Range of Solar Reflectances and Infrared Emittances Observed for Weathered Coatings, pp. 3.361-3.372, *Proceedings, 2000 Summer Study on Energy Efficiency in Buildings.* Washington, D.C.: American Council for an Energy-Efficient Economy.

Content of Tables

Table 1. Weathering Sites for Exposing Roof Products

Company	City	County	Climate Zone	Roof or Ground Mount
Department of Water Resources CIMIS	El Centro (RS01)	Imperial	15	Ground
Maruhachi Ceramics of America	Corona (RS02)	Riverside	10	Ground
BASF	Colton (RS03)	San Bernadino	10	Roof
ELK Corporation	Shafter (RS04)	Kern	13	Ground
Steelscape	Richmond (RS05)	Contra Costa	3	Roof
Custom-Bilt	Sacramento (RS06)	Sacramento	12	Roof
Department of Water Resources CIMIS	McArthur (RS07)	Shasta	16	Ground

Table 2. Sample Identifications and Solar Reflectance after 1.63 and 4.06 years of exposure.

	El Centro (RS01)	Corona (RS02)	Colton (RS03)	Shafter (RS04)	Richmond (RS05)	Sacramento (RS06)	McArthur (RS07)
CIMIS Site[1]	87	44	44	5	157	131 & 155	43
Latitude	32°48'24"N	33°57'54"N	33°57'54"N	35°31'59"N	37°59'30"N	38°35'58"N	41°03'53"N
Longitude	115°26'46"W	117°20'08"W	117°20'08"W	119°16'52"W	122°28'12"W	121°32'25"W	121°27'16"W
Samples for Element Study	Gray Artic concrete tile	Gray Artic concrete tile	PVDF Metal Charcoal Gray	PVDF Metal Rawhide	PVDF Metal Rawhide	Gray Artic concrete tile	PVDF Metal Rawhide
Sample ID	976	676	517,518,519	704, 705, 706, 707	404,406	378	805,806
Sample Area (m^2)	7.903E-03	7.903E-03	2.371E-02	3.161E-02	1.581E-02	7.903E-03	1.581E-02
SR initial	0.265	0.252	0.308	0.571	0.569	0.269	0.570
SR after 1.63 yrs	0.275	0.233	0.297	0.524	0.545	0.248	0.547
Samples for Biomass Study	PVDF Metal Hartford Green	PVDF Metal Charcoal Gray	Gray Artic concrete tile	Buff Blend Clay tile	PVDF Metal Rawhide	Brown Artic concrete tile	PVDF Metal Rawhide
Sample ID	920, 921, 922, 923	616	576	779,780	405	372	804,807
Sample Area (m^2)	3.161E-02	7.903E-03	7.903E-03	1.581E-02	7.903E-03	7.903E-03	1.581E-02
SR aged	0.272	0.309	0.246	0.527	0.569	0.261	0.571
SR after 1.63 yrs	0.277	0.297	0.241	0.484	0.544	0.254	0.549
Samples for Element Study	PVDF Metal Red Brick	PVDF Metal Hartford Green	PVDF Metal Slate Blue	MCA Clay Tile White Buff	PVDF Metal Rawhide	PVDF Metal Charcoal Gray	PVDF Metal Slate Blue
Sample ID	912-915	620-623	508-511	728-730	407	316-319	808-811
Sample Area (m^2)	3.161E-02	3.161E-02	3.161E-02	2.37E-02	7.90E-03	3.161E-02	3.161E-02
SR initial	0.374	0.272	0.283	0.636	0.440	0.308	0.282
SR after 4.06 yrs	0.405	0.340	0.274	0.442	0.424	0.282	0.267
	Clay Apricot Buff	Shepherd Gray Artic	MonierLife Terracotta red	Shepherd Blue Artic	MCA Clay Tile Weathered Green	Am Roof Coatings	MCA Clay Tile Regency Blue
Sample ID	931-933	677-678	549-551, 578	764-766	443-445	381-386	837-839
Sample Area (m^2)	2.37E-02	1.58E-02	3.16E-02	2.37E-02	2.37E-02	4.74E-02	2.37E-02
SR initial	0.608	0.247	0.199	0.236	0.415	See Below[2]	0.420
SR after 4.06 yrs	0.493	0.304	0.222	0.252	0.354		0.418

[1] http://wwwcimis.water.ca.gov/cimis/welcome.jsp

[2]Solar reflectance for Am Rooftile Coatings exposed in Sacramento, CA

Table 3. Thermal Emittance measured for roof coupons at different sites over time of exposure.

Roof Sample	Site	Thermal Emittance at Exposure Times (yrs)						
		0.000	0.748	0.962	1.630	2.493	3.592	4.055
Charcoal Gray PVDF Metal	**Corona**	0.83			0.82	0.84	0.84	0.83
	Richmond	0.82	0.82	0.82				
Rawhide PVDF Metal	**Corona**	0.86			0.84	0.87	0.84	0.85
	Richmond	0.83	0.84	0.84				
Apricot Buff Clay Tile	**Corona**	0.86	0.85	0.92	0.82	0.91	0.90	0.90
	Richmond	0.86	0.83	0.83				
Gray Artic Concrete Tile	**Corona**		0.84					
	Richmond		0.84	0.84				

Table 4. Derived OC and EC Amounts per Unit Area on the Roof Samples Collected at the CA Sites (Detection Limit of Carbon is 0.2 μg)

Site ID	Organic Carbon (mg/m^2)		Elemental Carbon (mg/m^2)	
	1.63 yr exposure	4.1 yr exposure	1.63 yr exposure	4.1 yr exposure
El Centro	8.312	NA	0.237	NA
Corona	5.361	52.226	0.240	0.987
Colton	6.146	54.565	0.165	2.833
Shafter	5.591	41.835	0.404	3.555
Richmond	11.090	8.745	1.344	0.569
Sacramento	4.461	NA	0.221	NA
McArthur	1.315	88.902	0.018	0.796

Table 5. Model Fitting for PVDF-painted Metal Coupons at All Slopes

Site	[.564,.764]			[.959,.962]			[1.625,1.644]		
	a	**r**	**sse**	**a**	**r**	**sse**	**a**	**r**	**sse**
Colton	0.0610	0.0540	0.0012	0.1480	0.1810	0.0056	0.0430	0.0130	0.0009
Corona	0.0320	0.0250	0.0004	0.0920	0.1020	0.0090	0.0440	0.0210	0.0014
Meloland	0.0390	0.0650	0.0024	0.0920	0.1650	0.0146	0.0080	0.0140	0.0009
McArthur	0.0190	0.0010	0.0005	0.0260	0.0310	0.0011	0.0170	0.0010	0.0007
Richmond	0.0770	0.0470	0.0012	0.0770	0.0470	0.0012	0.0210	0.0010	0.0005
Sacramento	0.0300	0.0010	0.0003	0.0640	0.0700	0.0015	0.0340	0.0050	0.0006
Shafter	0.1030	0.1020	0.0063	0.1210	0.1190	0.0069	0.0360	0.0010	0.0048
	[2.488,2.501]			**[3.589,3.592]**			**[4.041,4.060]**		
Colton	0.0620	0.0590	0.0022	0.0550	0.0470	0.0018	0.1610	0.1640	0.1170
Corona	0.0820	0.0950	0.0042	0.0600	0.0770	0.0032	0.2040	0.3300	0.0037
Meloland	0.0770	0.1580	0.0048	0.0660	0.1420	0.0064	0.0970	0.2120	0.0083
McArthur	0.0100	0.0200	0.0009	0.0080	0.0110	0.0006	0.0250	0.0300	0.0015
Richmond	0.0130	0.0150	0.0009	0.0230	0.0220	0.0029	0.0580	0.0430	0.0184
Sacramento	0.0370	0.0290	0.0012	0.0600	0.0340	0.0041	0.0900	0.0790	0.0050
Shafter	0.0830	0.0570	0.0056	0.0650	0.0550	0.0019	0.1210	0.1060	0.0140

Table 6. Model Fitting for Clay Tiles at All Slopes

Site	[.564,.764]			[.959,.962]			[1.625,1.644]		
	a	**r**	**sse**	**a**	**r**	**sse**	**a**	**r**	**sse**
Colton	0.0710	0.0400	0.0045	0.1390	0.1450	0.0040	0.0580	0.0010	0.0046
Corona	0.0530	0.0470	0.0034	0.1010	0.1100	0.0099	0.0800	0.0570	0.0033
Meloland (El Centro)	0.0700	0.1260	0.0031	0.0840	0.1830	0.0037	0.0540	0.1040	0.0035
McArthur	0.0210	0.0010	0.0033	0.0240	0.0310	0.0027	0.0210	0.0010	0.0027
Richmond	0.0590	0.0270	0.0032	0.0590	0.0270	0.0032	0.0460	0.0010	0.0035
Sacramento	0.0390	0.0050	0.0033	0.0580	0.0740	0.0038	0.0560	0.0260	0.0043
Shafter	0.1300	0.1430	0.0075	0.1440	0.1780	0.0103	0.0840	0.0430	0.0053
	[2.488,2.501]			**[3.589,3.592]**			**[4.041,4.060]**		
Colton	0.0990	0.0650	0.0039	0.0970	0.0630	0.0038	0.1970	0.2010	0.0216
Corona	0.1330	0.1590	0.0066	0.1280	0.1290	0.0142	0.2050	0.3000	0.0048
Meloland (El Centro)	0.0940	0.2000	0.0033	0.1070	0.2410	0.0021	0.1270	0.2820	0.0039
McArthur	0.0160	0.0270	0.0021	0.0180	0.0120	0.0027	0.0140	0.0140	0.0037
Richmond	0.0490	0.0260	0.0035	0.0690	0.0310	0.0029	0.0850	0.0450	0.0051
Sacramento	0.0550	0.0480	0.0066	0.1110	0.0840	0.0070	0.1310	0.1270	0.0103
Shafter	0.1390	0.1090	0.0042	0.1100	0.0920	0.0050	0.1780	0.1930	0.0043

Table 7. Chemical Concentration (mg m^{-2}) of Particulate Matter

		1.6 Years					4 YEARS				
Site #		**RS02**	**RS03**	**RS04**	**RS05**	**RS07**	**RS02**	**RS03**	**RS04**	**RS05**	**RS07**
Site Name		**Corona**	**Colton**	**Shafter**	**Richmond**	**McArthur**	**Corona**	**Colton**	**Shafter**	**Richmond**	**McArthur**
Latitude, Longitude		**33.88N, 117.56W**	**34.07N, 117.31W**	**35.5N, 119.27W**	**37.94N, 122.34W**	**41.02N, 121.65W**	**33.88N, 117.56W**	**34.07N, 117.31W**	**35.5N, 119.27W**	**37.94N, 122.34W**	**41.02N, 121.65W**
Soil Absorption a		**0.06**	**0.053**	**0.058**	**0.034**	**0.019**	**0.206**	**0.177**	**0.147**	**0.075**	**0.02**
Soil Reflectance r		**0.03**	**0.014**	**0.012**	**0.001**	**0.001**	**0.315**	**0.173**	**0.128**	**0.049**	**0.026**
Aluminum	**Al**	41.00	39.06	16.45	26.70	5.35	27.42	9.91	14.44	12.38	8.07
Barium	**Ba**	0.71	0.52	0.48	0.26	0.23	0.52	0.00	0.33	0.47	0.27
Calcium	**Ca**	55.29	95.74	17.33	146.14	1.01	30.88	39.89	42.51	8.64	4.01
Chromium	**Cr**	0.63	0.74	1.30	0.80	0.69	5.71	4.38	2.64	0.95	0.32
Copper	**Cu**	1.44	1.13	0.75	0.94	0.29	0.26	0.10	0.24	0.18	0.15
Iron	**Fe**	67.44	67.06	31.63	43.97	4.95	51.09	23.54	28.65	29.56	9.53
Lead	**Pb**	0.36	0.47	0.09	0.00	0.00	0.14	0.09	0.06	0.14	0.03
Magnesium	**Mn**	19.74	19.78	9.02	15.50	0.51	1.41	0.23	1.43	0.46	0.12
Nickel	**Ni**	0.00	0.29	0.09	0.20	0.00	0.07	0.00	1.53	0.13	0.02
Potassium	**K**	10.26	9.66	3.23	0.00	0.00	9.49	5.08	7.63	5.88	2.12
Silicon	**Si**	19.11	13.71	6.83	9.68	2.33	39.32	20.29	28.44	36.34	18.80
Strontium	**Sr**	0.49	0.17	0.64	0.21	0.18	0.25	0.21	0.18	0.16	0.08
Sulfur	**S**	1.80	1.73	1.35	1.75	0.00	0.00	0.46	0.54	0.47	0.05
Titanium	**Ti**	4.11	3.28	0.96	2.31	0.20	2.31	1.60	1.75	2.51	1.68
Zinc	**Zn**	4.38	1.35	7.28	1.13	3.18	0.97	0.47	0.82	0.48	0.16
Organic Carbon	**OC**	5.36	6.15	5.59	11.09	1.32	52.23	54.56	41.83	8.74	88.90
Elemental Carbon	**EC**	0.24	0.17	0.40	1.34	0.02	0.99	2.83	3.55	0.57	0.80

Table 8. Major Rotated Eigenvectors of Correlation with Soil Properties

PCA for soil absorptance a				PCA for soil reflectance r			
	1st	2nd	3rd		1st	2nd	3rd
a	0.000	0.000	0.000	**r**	0.000	0.000	0.000
Al	1.340	-2.171	1.645	**Al**	1.340	-2.171	1.645
Ba	0.000	-0.001	0.000	**Ba**	0.000	-0.001	0.000
Ca	9.759	46.866	-1.908	**Ca**	9.759	46.866	-1.908
Cr	-0.543	-0.476	-0.504	**Cr**	-0.544	-0.476	-0.504
Cu	0.000	0.000	0.000	**Cu**	0.000	0.000	0.000
Fe	91.639	105.473	39.203	**Fe**	91.639	105.473	39.203
Pb	0.000	0.000	0.000	**Pb**	0.000	0.000	0.000
Mn	-0.277	-1.792	-0.822	**Mn**	-0.276	-1.791	-0.821
Ni	0.000	0.000	0.000	**Ni**	0.000	0.000	0.000
K	0.000	0.001	0.000	**K**	0.000	0.001	0.000
Si	-2.203	-5.381	-3.305	**Si**	-2.203	-5.381	-3.305
Sr	0.000	0.000	0.000	**Sr**	0.000	0.000	0.000
S	-0.389	-0.414	-0.400	**S**	-0.390	-0.415	-0.401
Ti	0.000	0.000	0.000	**Ti**	0.000	0.000	0.000
Zn	0.450	-0.773	6.400	**Zn**	0.450	-0.773	6.400
OC	-41.437	-50.573	-14.278	**OC**	-41.437	-50.573	-14.278
EC	-0.621	0.890	-0.180	**EC**	-0.621	0.889	-0.180

Table 9. Best Models for Predicting a and r

	1.6+4y		1-element		2-elements		3-elements	
Abbr.	**a**	**r**	**a**	**r**	**a**	**r**	**a**	**r**
b	0.0000	0.0000	0.0133	-0.0281	0.0016	0.0021	0.0013	-0.0732
Al	0.0024	-0.0586	0.0000	0.0000	0.0000	0.0000	0.0000	0.0000
Ba	-0.0003	0.0072	0.0000	0.0000	0.0000	0.0000	0.0000	0.0000
Ca	0.0000	0.0000	0.0000	0.0000	0.0000	0.0000	0.0000	0.0000
Cr	0.0001	-0.0003	0.0350	0.0540	-0.0067	-0.0544	-0.0091	-0.0214
Cu	0.0319	0.0320	0.0000	0.0000	0.0000	0.0000	0.0000	0.0000
Fe	0.0000	0.0000	0.0000	0.0000	0.0000	0.0000	0.0000	0.0395
Pb	-0.0016	0.0030	0.0000	0.0000	0.0000	0.0000	0.0000	0.0000
Mn	0.0000	0.0000	0.0000	0.0000	0.0000	0.0000	0.0000	0.0000
Ni	0.0027	-0.0154	0.0000	0.0000	0.0000	0.0000	0.0000	0.0000
K	0.0000	0.0000	0.0000	0.0000	0.0000	0.0000	0.0289	0.0000
Si	0.0052	-0.0090	0.0000	0.0000	0.0290	0.0461	0.0015	0.0000
Sr	0.0017	-0.0012	0.0000	0.0000	0.0000	0.0000	0.0000	0.0000
S	0.0000	0.0000	0.0000	0.0000	0.0000	0.0000	0.0000	0.0022
Ti	0.0000	0.0000	0.0000	0.0000	0.0000	0.0000	0.0000	0.0000
Zn	0.0000	0.0000	0.0000	0.0000	0.0000	0.0000	0.0000	0.0000
OC	-0.0008	-0.0017	0.0000	0.0000	0.0000	0.0000	0.0000	0.0000
EC	-0.0002	0.0004	0.0000	0.0000	0.0000	0.0000	0.0000	0.0000

Table 10. Comparison of Measurements with Literature Data

Absorbing Species	Absorption coefficient from our data (m^2 g^{-1})	Absorption coefficient, estimate is from literature (m^2 g^{-1})
Fe	1.5	0.2 – 1.0
Cr	20.	–
EC	16	8, 11

Caption of Figures

Fig. 1 Assembly used for natural exposure testing of roof samples in seven California climatic zones; site shown is the GAF/Elk Manufacturing facility in Shafter, CA.

Fig. 2 Solar reflectance of PVDF metal (white color) at the seven CA weathering sites.

Fig. 3 Painted PVDF metal coupon soiled at the Shafter site after 1 full year of exposure.

Fig. 4 Solar reflectance of a painted PVDF metal coupon (charcoal gray color) at the seven CA weathering sites.

Fig. 5 Solar reflectance of a concrete tile coupon (Terra Cotta Red color) at the CA sites.

Fig. 6 Regal white painted metal with and without cool pigments. The slopes of 9.5º, 18.4º and 33.7º represent respective exposure settings of 5.08-cm, 10.16-cm and 20.32-cm of rise per 30.48-cm of run.

Fig. 7 Elemental compositions and carbon contents of particulate matter extracted from roof samples during March 2005. Samples exposed for 1.63 years.

Fig. 8 Elemental compositions and carbon contents of particulate matter extracted from roof samples during August 2007. Samples exposed for 4.06 years.

Fig. 9 Diagram showing photon behavior for retained terms in the expansion for the soiled substrate reflectance R.

Fig. 10 The measured solar reflectance R is compared to the modeled R as computed from linear regression of the a and r terms (Eq. 2).

Fig. 11 Estimation of soil absorptance a based on absorber concentrations. Data from Table 7 for 4 yr. Fit lines are required to pass through the origin. Parameters of the linear relationships were selected by minimizing the root mean square deviation Δa of the points from the line. In part (a) only iron concentration [Fe] was considered, in part (b) Fe and Cr, and in part (c) Fe, Cr, and elemental carbon C were all considered.

Fig. 1. Assembly used for natural exposure testing of roof samples in seven California climatic zones; site shown is the GAF/Elk Manufacturing facility in Shafter, CA.

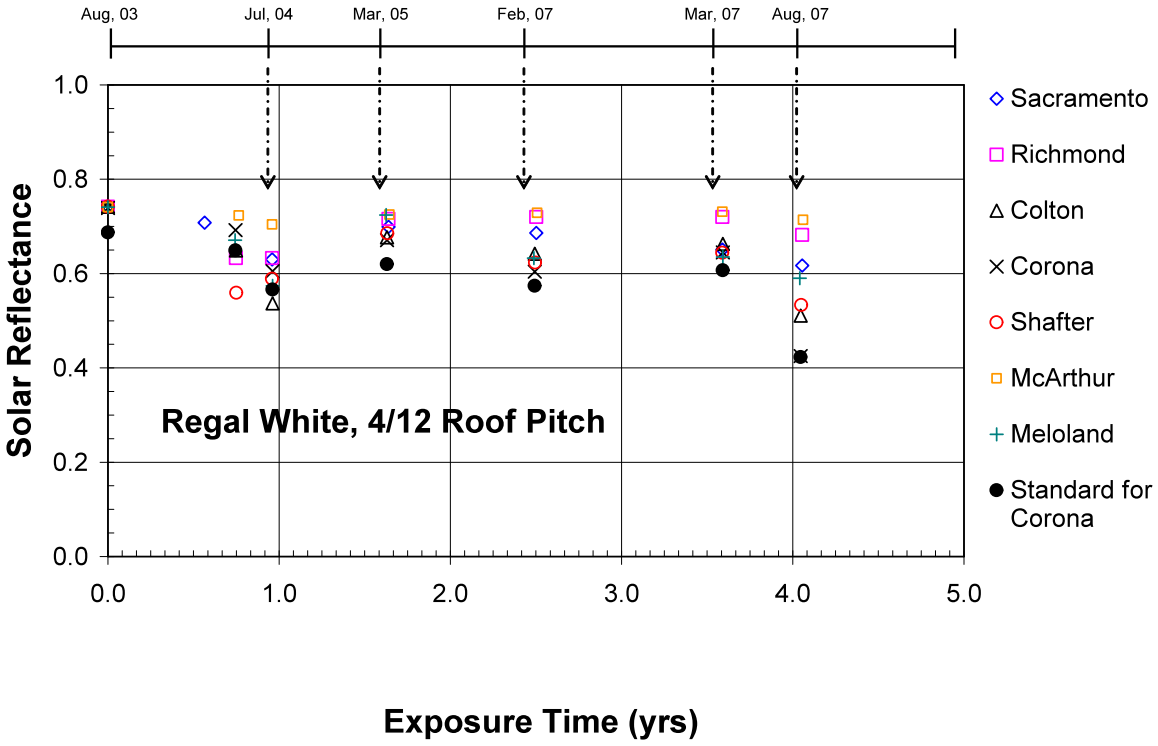

Fig. 2. Solar reflectance of PVDF metal (white color) at the seven CA weathering sites.

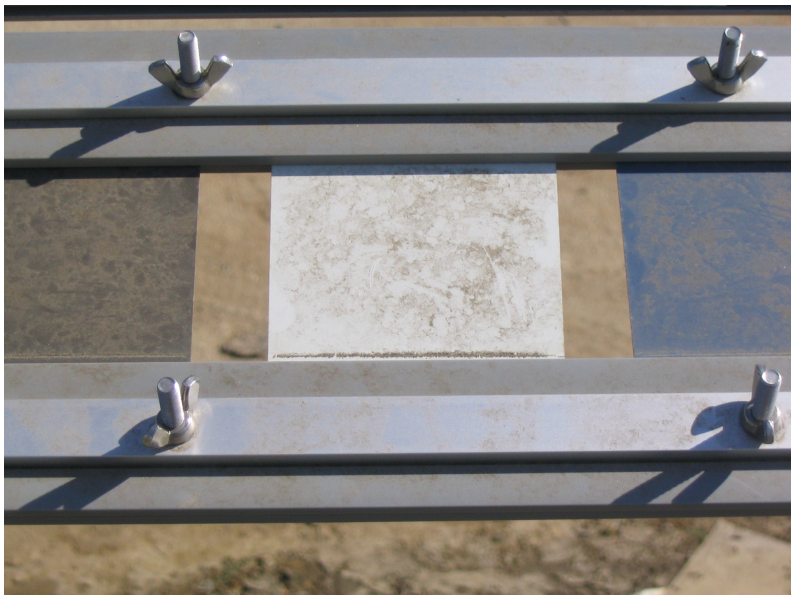

Fig. 3. Painted PVDF metal coupon soiled at the Shafter site after 1 full year of exposure.

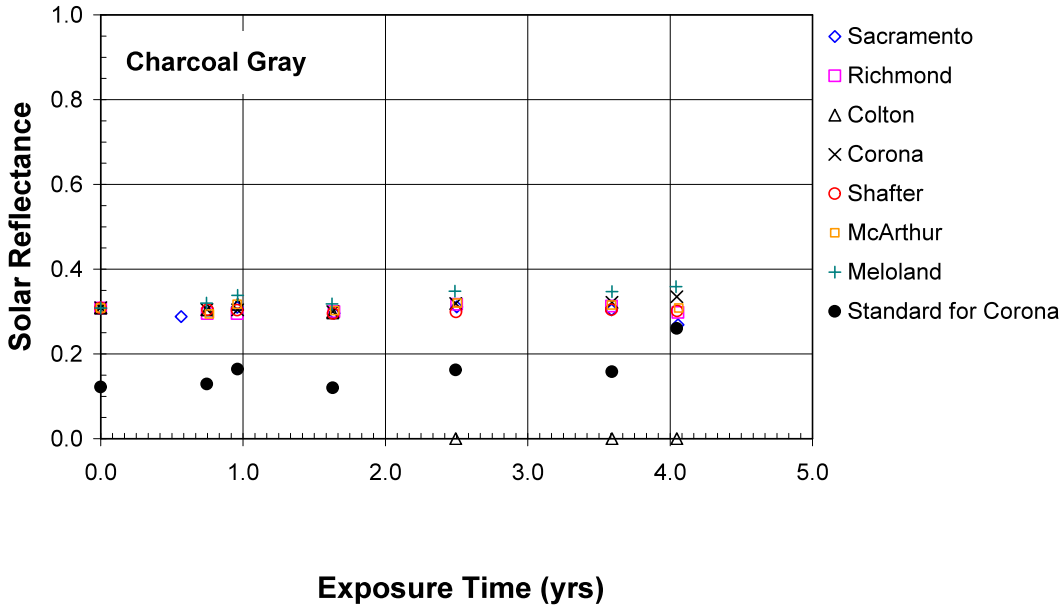

Fig. 4. Solar reflectance of a painted PVDF metal coupon (charcoal gray color) at the seven CA weathering sites.

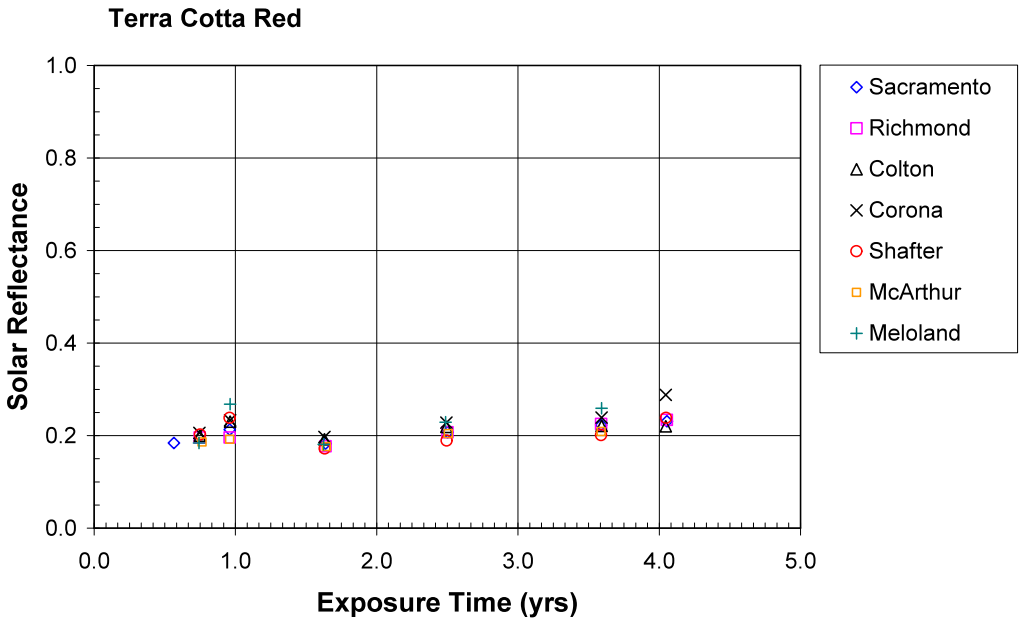

Fig. 5. Solar reflectance of a concrete tile coupon (Terra Cotta Red color) at the CA sites.

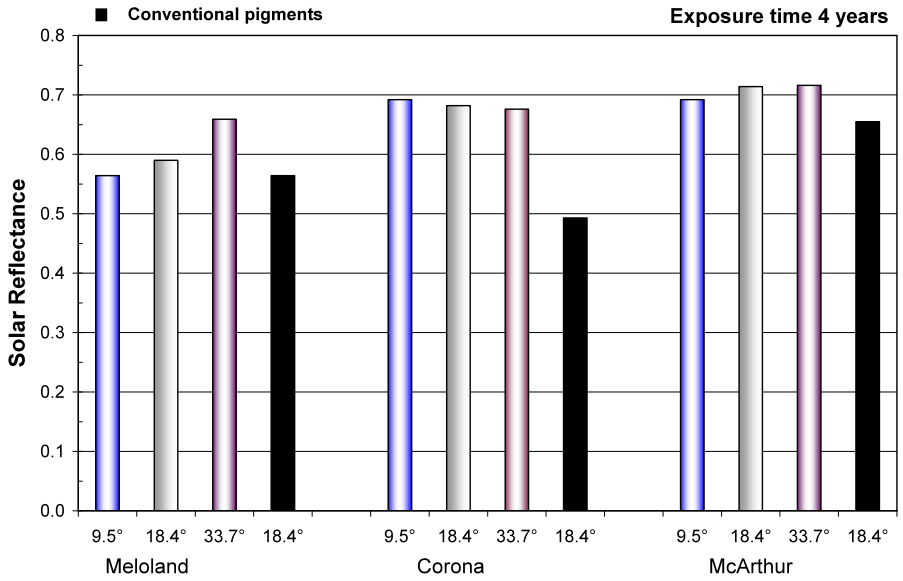

Fig. 6. Regal white painted metal with and without cool pigments. The slopes of 9.5º, 18.4º and 33.7º represent respective exposure settings of 5.08-cm, 10.16-cm and 20.32-cm of rise per 30.48-cm of run.

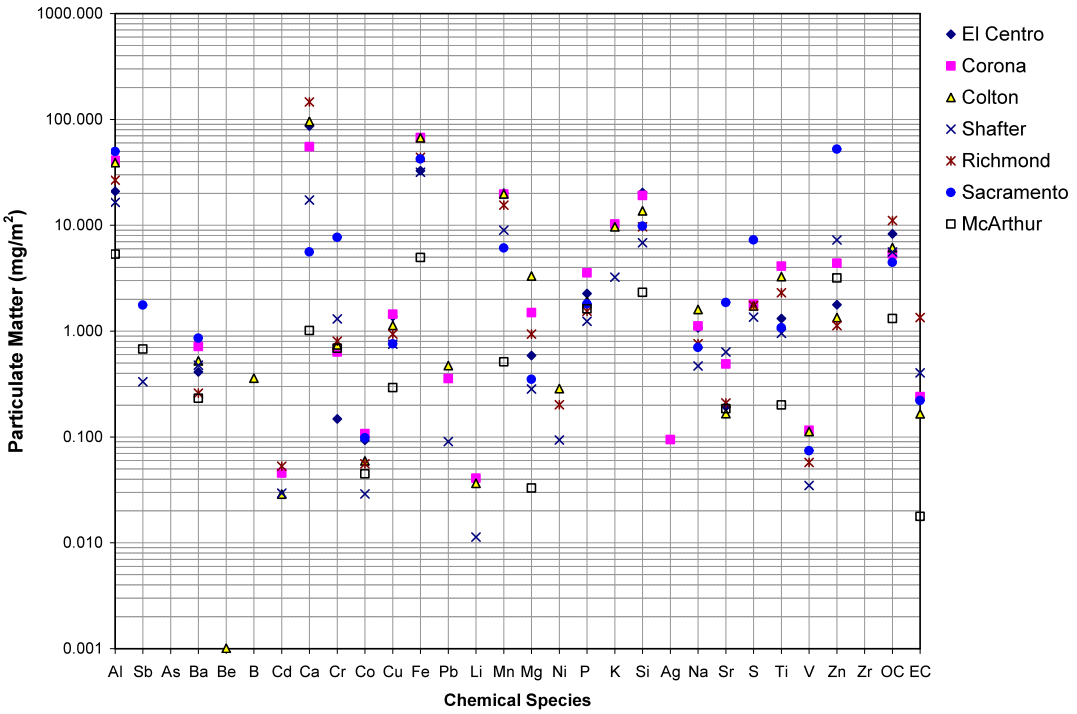

Fig. 7. Elemental compositions and carbon contents of particulate matter extracted from roof samples during March 2005. Samples exposed for 1.63 years.

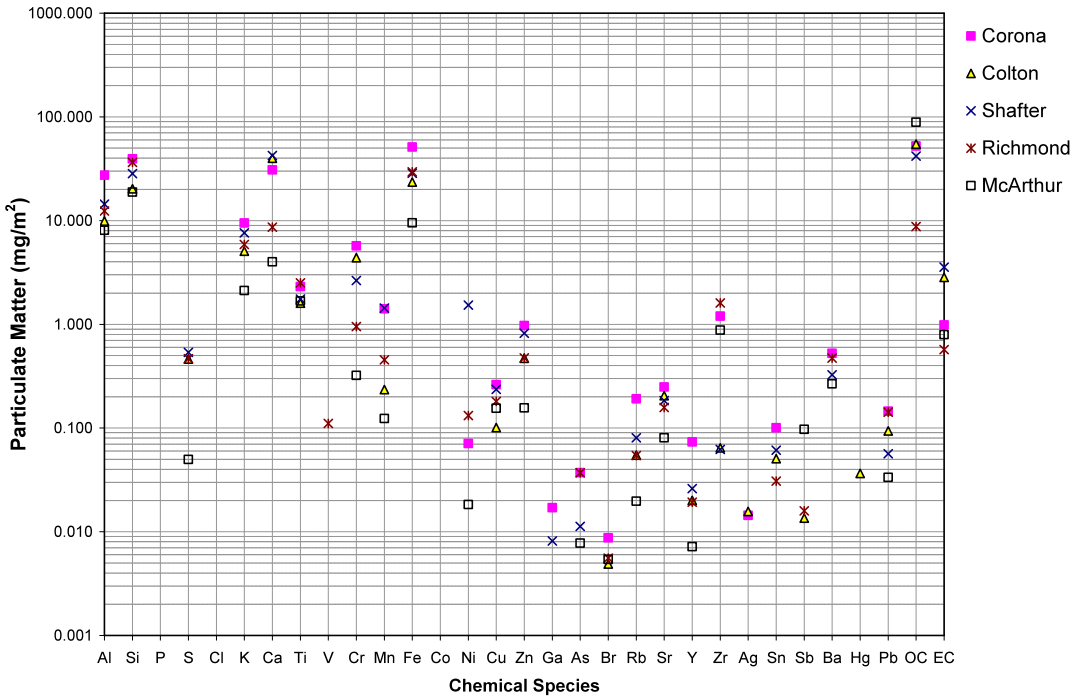

Fig. 8. Elemental compositions and carbon contents of particulate matter extracted from roof samples during August 2007. Samples exposed for 4.06 years.

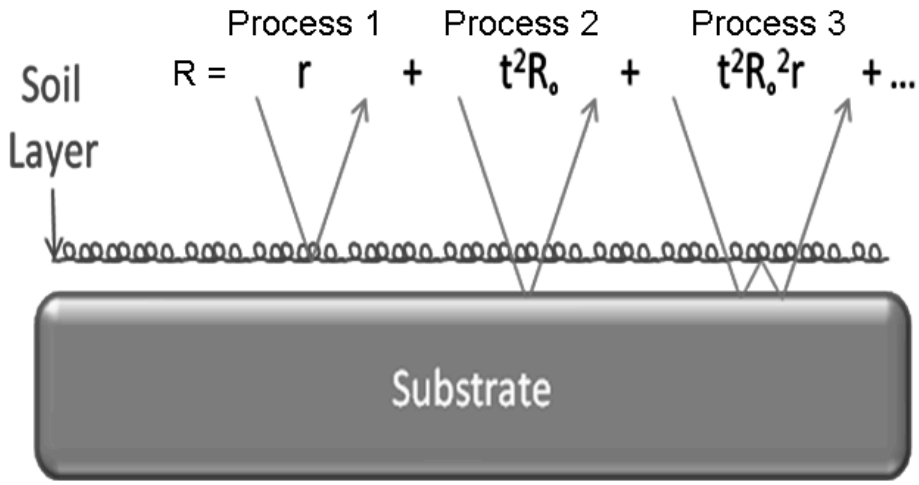

Fig. 9. Diagram showing photon behavior for retained terms in the expansion for the soiled substrate reflectance R.

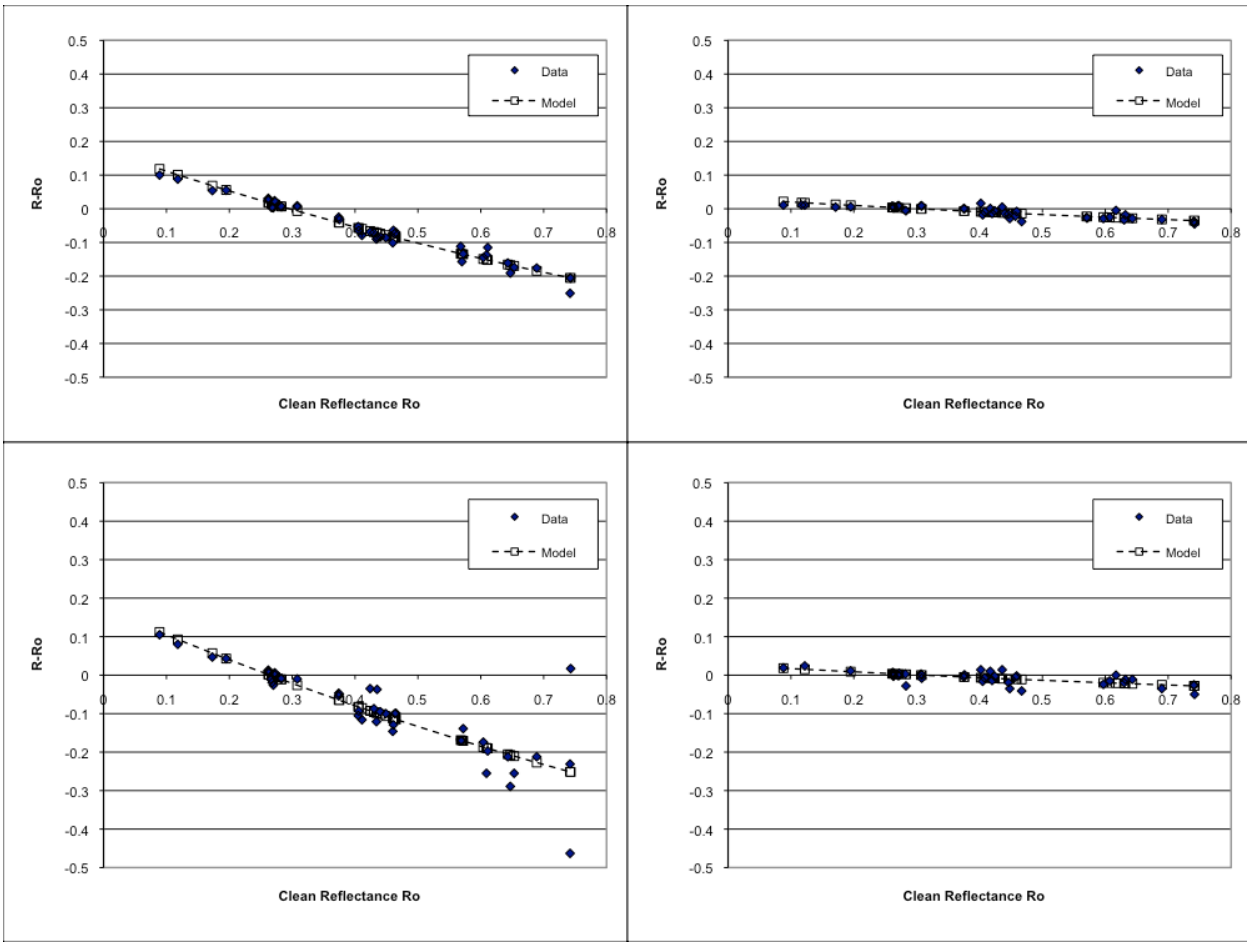

Fig. 10. The measured solar reflectance R is compared to the modeled R as computed from linear regression of the *a* and *r* terms (Eq. 2).

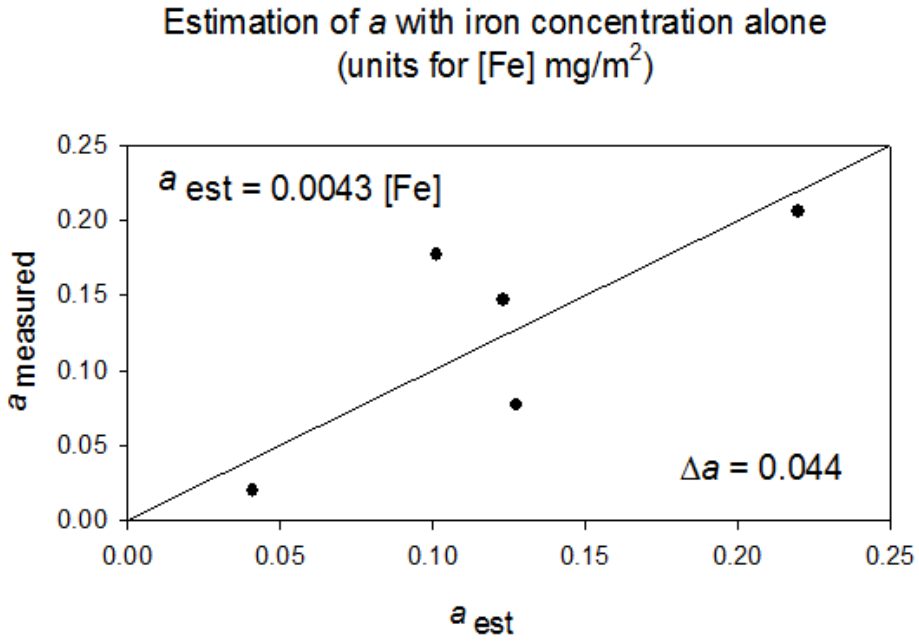

Fig. 11(a)

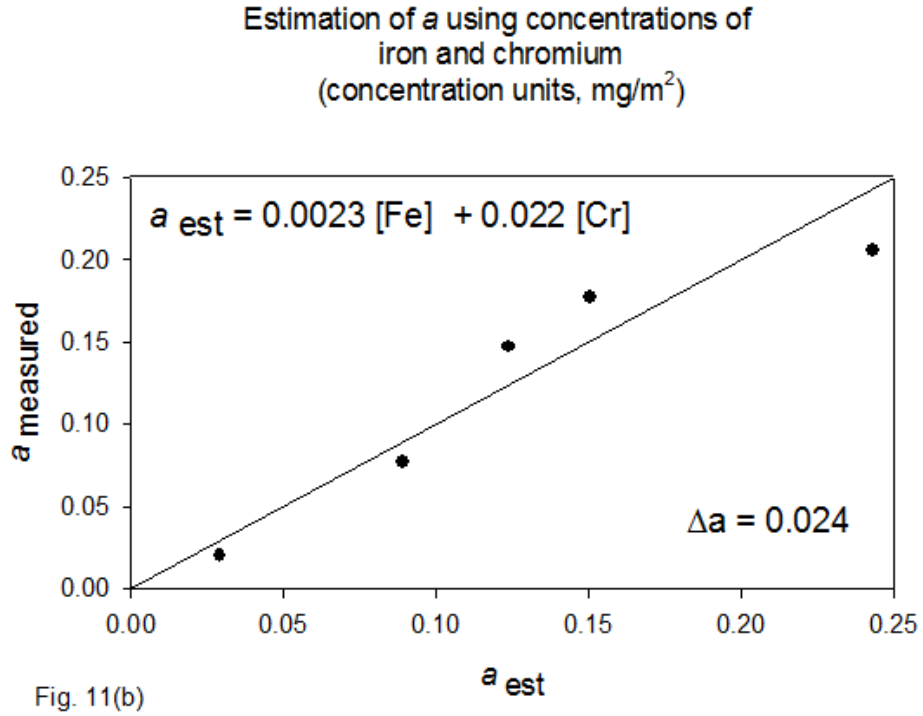

Fig. 11(b)

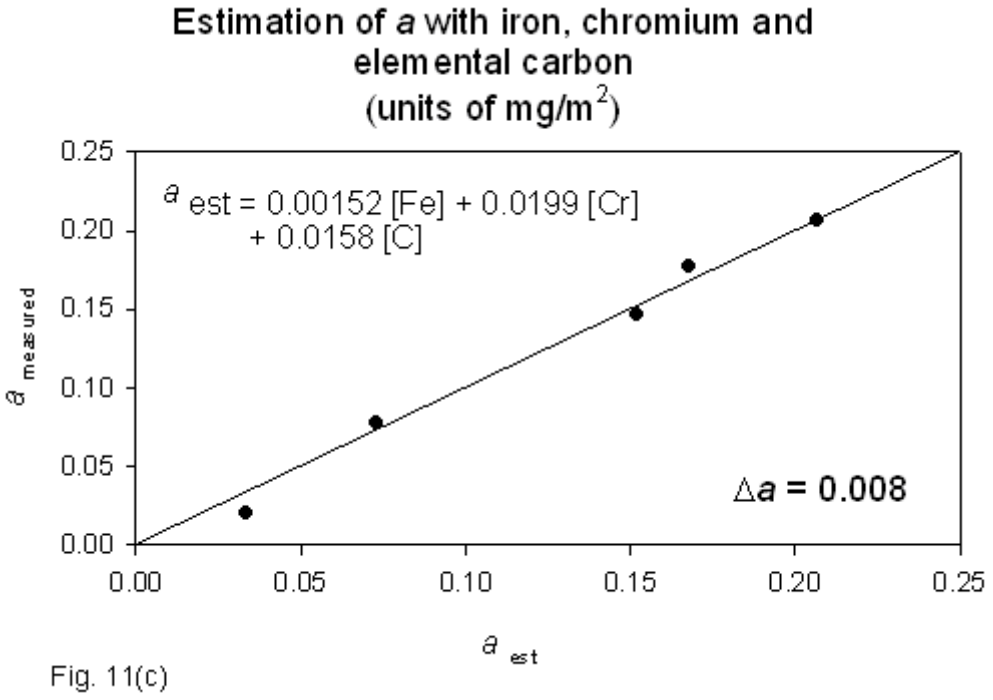

Fig. 11(c)

Fig. 11. Estimation of soil absorptance *a* based on absorber concentrations. Data from Table 7 for 4 yr. Fit lines are required to pass through the origin. Parameters of the linear relationships were selected by minimizing the root mean square deviation Δa of the points from the line. In part (a) only iron concentration [Fe] was considered, in part (b) Fe and Cr, and in part (c) Fe, Cr, and elemental carbon C were all considered.